

Complex Meson Spectroscopy

Eef van Beveren*, Frieder Kleefeld† and George Rupp†

*Centro de Física Teórica, Departamento de Física, Universidade, P3004-516 Coimbra, Portugal

†Centro de Física das Interacções Fundamentais, Instituto Superior Técnico, Edifício Ciência, P1049-001 Lisboa, Portugal

Abstract. We do meson spectroscopy by studying the behavior of S -matrix poles in the complex-energy plane, as a function of the coupling strength for 3P_0 quark-pair creation. Thereto, a general formula for non-exotic hadron-hadron scattering involving arbitrary quark confinement is used, which can be applied to all flavors. We find two distinct types of poles, which we call *confinement* and *continuum* poles, respectively. Together, they suffice to understand the experimental meson spectrum.

Introduction. From past studies on atomic spectra, we got so used to the terms “line spectrum” and “states” that we also apply them to mesonic spectra. Such a situation is depicted in Fig. 1a. The decay widths are thought of as higher-order effects, which indicate the life times of unstable states. This is indeed a fruitful strategy for atomic spectra. Starting from QED, one first determines the properties of the force which binds electrons to the nucleus, and next the corresponding bound-state spectra and states. Subsequently, one determines life times of states by considering the electromagnetic

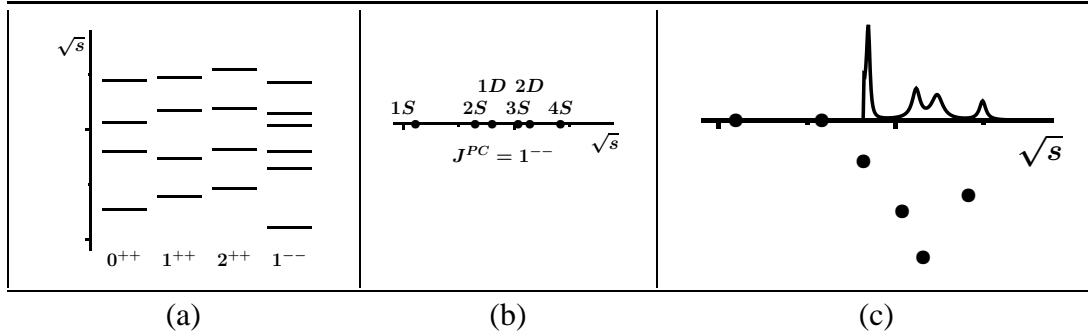


FIGURE 1. (a): Spectra as we are used to. (b): The same, but restricted to one set of quantum numbers. (c): A modern spectrum of bound states below and resonances above threshold, in terms of complex poles of the scattering amplitude (Note that the units along the real and the imaginary axis are not the same in this figure).

(EM) interaction of the photon field with the electrons.

Seen from a different angle, the above strategy amounts to separating the interaction of electrons and the nucleus with the EM field into two distinct parts: the one binding electrons and the nucleus into an atom, and the one describing the scattering of photons off the atom.

Here, we apply the same technique to strong interactions, but with the important difference that no manageable scheme exists to disentangle the two parts when setting

out from QCD. Hence, they must be dealt with on the same footing. As a consequence, also the central resonance position and the resonance width must be described on the same footing, which can be achieved by referring to the complex pole position of the corresponding scattering amplitude. Such situation is depicted in Fig. 1c.

Furthermore, the term “states” is not very well defined for resonances having large widths compared to their level separations. One may, of course, refer to the state at a certain energy, say the central resonance position. But it is not reasonable to assume that at energies say 100 MeV higher or lower, the state of the system is the same. Moreover, different resonances may be overlapping.

Here, we shall be studying non-exotic meson-meson scattering. Through quark-pair creation, this implies multi-channel scattering, as well as intermediate states of confined systems of quarks and antiquarks. Hence, the advantage of complex spectra is apparent, since the pole structure of the full scattering matrix is the same for all channels, although the structure of peaks and zeros in the various channels can be very different.

Meson-meson scattering amplitude. On rather general grounds [1, 2], it can be shown that a system of confined quarks and antiquarks coupled to free two-meson channels is well described by a partial-wave (ℓ) inverse cotangent matrix of the form

$$K_\ell(p) = \frac{\lambda^2 \sum_{n=0}^{\infty} \frac{\mathcal{J}_{n\ell}^*(p) \mathcal{J}_{n\ell}(p)}{E(p) - E_{n\ell}}}{\lambda^2 \sum_{n=0}^{\infty} \frac{\mathcal{J}_{n\ell}^*(p) \mathcal{N}_{n\ell}(p)}{E(p) - E_{n\ell}} - 1} . \quad (1)$$

Here, λ parametrizes the intensity of quark-pair creation, p stands for the relativistic relative on-shell momentum in one of the two-meson channels, and $E(p)$ is the total invariant mass of the system. Furthermore, $E_{n\ell}$ ($n = 0, 1, \dots$) represent the *confinement spectrum*, which is of course model-dependent, since it cannot be measured directly, while $\mathcal{J}_{n\ell}$ and $\mathcal{N}_{n\ell}$ are convolution matrix integrals over quark-antiquark distributions, meson-meson scattering wave functions, and a transition potential.

If we approximate the latter potential by a radial delta function, then we find for the ij -th matrix element of the partial-wave scattering amplitude

$$[T_\ell]_{ij}(p) = \frac{\lambda^2 \left\{ \sum_{n=0}^{\infty} \frac{r_i(n) r_j(n)}{\sqrt{s} - E_{n\ell}} \right\} 2a \sqrt{\frac{\mu_i \mu_j}{p_i p_j}} p_i p_j j_{\ell_i}(p_i a) j_{\ell_j}(p_j a)}{1 + \lambda^2 \sum_{m=1}^N \left\{ \sum_{n=0}^{\infty} \frac{|r_m(n)|^2}{\sqrt{s} - E_{n\ell}} \right\} 2ia \mu_m p_m j_{\ell_m}(p_m a) h_{\ell_m}^{(1)}(p_m a)} . \quad (2)$$

Here, j_ℓ represents the radial Bessel function, $h_\ell^{(1)}$ the radial Hankel function of the first kind, a the delta-shell radius, \sqrt{s} the total invariant mass of the system, and μ_i the reduced mass in the i -th two-meson channel. The coefficients $r_i(n)$ (*vertex functions*), which stem from the convolution integrals, are discussed later.

Cross sections and poles. In Fig. 2 we show how cross sections following from formula (2) vary with increasing λ , for S -wave isodoublet $K\pi$ scattering. In Fig. 2a

the nonstrange-strange ($n\bar{s}$) confinement spectrum is well visible for small λ , whereas in Fig. 2c, for the model value of λ , experiment is reproduced.

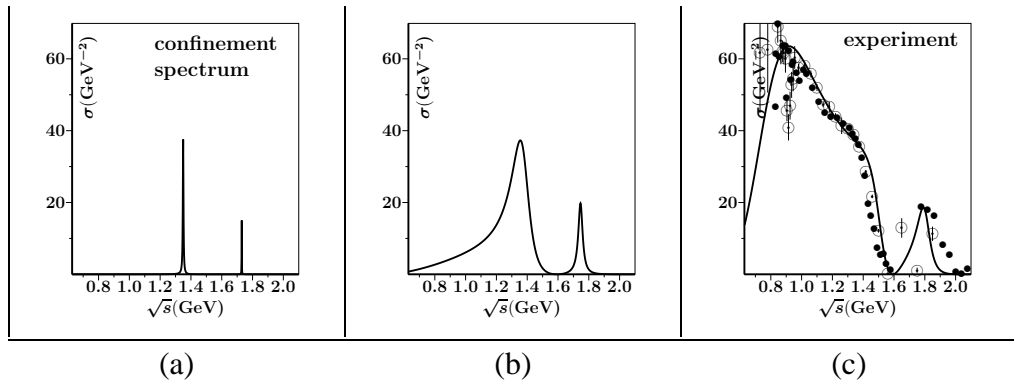


FIGURE 2. Cross section for S -wave isodoublet $K\pi$ scattering. Left: For very small values of λ , one observes the $J^{PC} = 0^{++}$ $n\bar{s}$ confinement spectrum. Middle: When λ takes about half its model value, one notices some more structure for low invariant masses. Right: At the model's value of λ , this structure is dominant and well in agreement with the experimental observations. The data are taken from Ref. [3] (open circles) and Ref. [4] (full circles).

The pole structure for varying λ is depicted in Fig. 3. In Fig. 3a we see how the pole stemming from the ground state of the confinement spectrum moves through the complex-energy ($E = \sqrt{s}$) plane when λ changes. The pole movement shown in Fig. 3b is very different. For small λ the pole disappears into the $K\pi$ continuum, which is the reason why it is not visible in Fig. 2a.

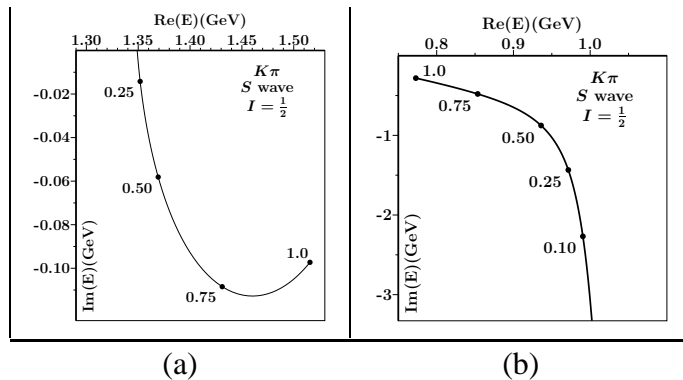


FIGURE 3. Pole positions for S -wave isodoublet $K\pi$ scattering, as a function of the strength of quark-pair creation, parametrized by λ (see Eqs. (1,2)). (a): Example of a *confinement pole*, which for $\lambda = 0$ lies on the real axis at total invariant mass $E_{0\ell}$, i.e., the ground state of the $n\bar{s} J^P = 0^+$ confinement spectrum. (b): Example of a *continuum pole*, which for $\lambda = 0$ has an infinite negative imaginary part, i.e., the $K\pi$ continuum.

The lowest-lying scattering-amplitude poles for DK in $J^P = 0^+$ and D^*K in $J^P = 1^+$ are shown in Fig. 4. The two poles in Fig. 4a represent the $D_{s0}^*(2317)$ resonance, which, in the absence of isospin-violating processes, comes out on the real axis, plus a broad resonance at about 2.8–2.9 GeV, undetected so far.

The two poles shown in Fig. 4b represent the $D_{s1}(2460)$ and $D_{s1}(2536)$ resonances, which both come out on the real axis.

In Fig. 4a we depict two possible alternatives (one pair of solid lines and one pair of dashed lines). They result from very small variations in the delta-shell radius. Consequently, it is not at all trivial how to connect experimental poles with either confinement or continuum poles.

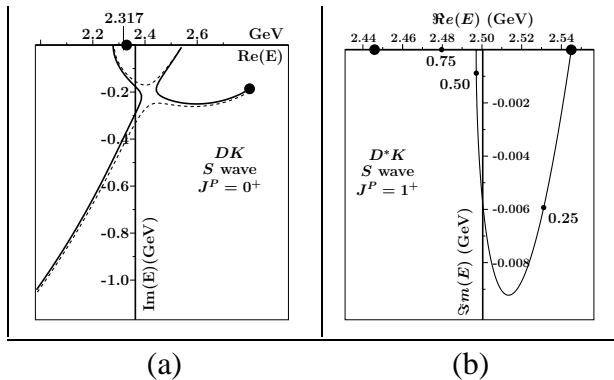


FIGURE 4. The lowest-lying poles for S -wave $J^P = 0^+$ DK (a) and $J^P = 1^+$ D^*K (b) scattering. The fat dots represent the pole positions for the model value of λ .

The two poles in Fig. 4b both stem from the ground state of the $J^P = 1^+$ charm-strange confinement spectrum, since there are two such states, i.e., 3P_1 and 1P_1 , which come out degenerate in our confinement spectrum. The linear combination 33% 3P_1 plus 67% 1P_1 decouples from D^*K S -wave scattering, hence becomes a bound state in the scattering continuum (see also Ref. [5]). On the other hand, the orthogonal linear combination of 3P_1 and 1P_1 couples fully, and turns into a bound state below threshold.

Threshold behavior. One may wonder how the lowest poles in Fig. 4 move along the real axis when λ is increased. This is depicted in Fig. 5, where we continuously vary λ

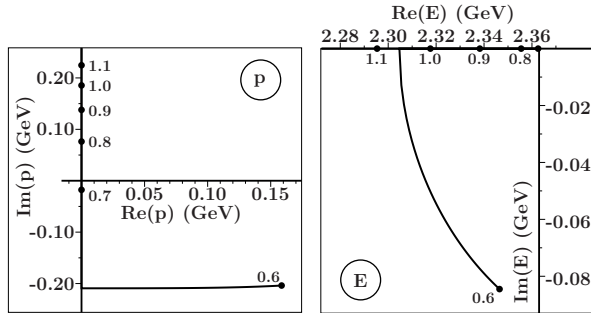


FIGURE 5. Movement of the $D_{s0}^*(2317)$ pole in S -wave DK scattering near the DK threshold, as a function of λ . Left: Movement in the p plane. Right: Movement in the E plane. We have marked the places where λ equals 0.6, 0.7, 0.8, 0.9, 1.0, and 1.1. On the real axis in the E plane, the pole moves first towards threshold and then towards smaller E for increasing λ .

from a small (0.60) towards a large value (1.2). In the complex-momentum (p) plane, we observe that the pole turns purely imaginary somewhere in the lower half-plane. This is typical for S -wave scattering. For any higher angular momentum this happens at $p = 0$. The S -matrix pole represents a bound-state when it lies on the positive imaginary axis.

On the negative imaginary axis, it represents a virtual bound state. In this example, the pole lies on top of threshold for a value of λ slightly larger than 0.7.

The pole position in the E plane can be obtained from the pole position in the p plane through the relation

$$E = \sqrt{p^2 + m_D^2} + \sqrt{p^2 + m_K^2} .$$

Properties. The properties of the scattering amplitude following from the K matrix of Eq. (1) are the following.

- Analytic in the total invariant mass.
- Proper analytical and smooth behavior at all thresholds.
- Unitary for real total invariant mass above and below thresholds.
- Symmetric for any complex value of the total invariant mass.
- Poles in the scattering matrix may be searched for in the same fashion as poles in any analytical function.
- It contains an infinity of interfering resonances.
- It also allows an arbitrary number (N) of coupled meson-meson channels.
- For small λ it exhibits the confinement spectrum $E_{n\ell}$.
- For the model's value of λ , it reproduces the resonances and bound states of meson-meson scattering.
- It contains kinematical Adler-type zeros [6] at almost the same invariant masses as the theoretical Adler zeros [7].
- It also reproduces automatically the low-lying scalar mesons.

The parameters. The parameters λ , a , and ω in formula (2) represent the probability of quark-pair creation, taken equal for up, down, strange and zero for the heavy flavors in the present version of the model, the average distance for quark-pair creation, and the average level spacing of the $q\bar{q}$ confinement spectrum, respectively. As expected, a is of the order of half a fermi, and ω of the order of 200 MeV. In principle, λ , a , and ω should follow from QCD. Furthermore, in our expression

$$E_{n\ell} = m_q + m_{\bar{q}} + \omega (2n + \ell + \frac{3}{2}) , \quad (3)$$

for the confinement spectrum, we must specify the constituent quark masses. We employ here the values $m_n = 0.406$ GeV, $m_s = 0.508$ GeV, $m_c = 1.562$ GeV, and $m_b = 4.724$ GeV from Ref. [1].

Moreover, flavor invariance demands that λ^2 and a^2 be scaled by the flavor mass, or the reduced quark mass in the case of different flavors [8, 9]. Consequently, for quark-pair creation, the average distance and probability decrease with increasing quark mass, as one naively would expect.

Sum rules for vertex functions. The vertex functions, represented by $r_i(n)$ in formula (2), where i indicates the channel index and n the radial excitation of the intermediate resonance, contain the full structure of all quantum numbers, with no parameters

involved. The former can be determined from the recoupling matrix elements of the harmonic-oscillator wave functions for the effective quarks. The complete procedure is described in Refs. [10], assuming the 3P_0 mechanism for quark-pair creation.

Some of the resulting vertex functions are shown in Table 1, for a system with quantum numbers $J^{PC} = 0^{++}$. Each of the two scattering products (mesons) is characterized

TABLE 1. Recoupling coefficients as a function of radial excitation n , for scalar ($J = 0, \ell = 1, S = 1, n$) decay into two mesons. Notice that the recoupling coefficients for $n = 0$ add up to one. This means that, in the harmonic-oscillator approach, there are no additional two-meson channels which can couple to the ground state of the confinement spectrum. For the higher radial excitations, the table is still very incomplete.

meson 1	meson 2	relative	recoupling coefficients
$(nJLS)_1 (J^{PC})$	$(nJLS)_2 (J^{PC})$	LS	$\{r(n)\}^2 \times 4^n$
$(0,0,0,0) (0^{-+})$	$(0,0,0,0) (0^{-+})$	$0,0$	$\frac{1}{24}(n+1)$
$(0,0,0,0) (0^{-+})$	$(1,0,0,0) (0^{-+})$	$0,0$	$\frac{1}{144}(2n+3)(n-1)^2$
$(1,0,0,0) (0^{-+})$	$(1,0,0,0) (0^{-+})$	$0,0$	$\frac{1}{3456}n(2n+1)(2n+3)(n-3)^2$
$(0,0,0,0) (0^{-+})$	$(0,1,1,1) (1^{++})$	$1,1$	$\frac{1}{6}$
$(0,1,0,1) (1^{--})$	$(0,1,0,1) (1^{--})$	$0,0$	$\frac{1}{72}(n+1)$
$(0,1,0,1) (1^{--})$	$(0,1,0,1) (1^{--})$	$2,2$	$\frac{1}{18}(2n+5)$
$(0,1,0,1) (1^{--})$	$(1,1,0,1) (1^{--})$	$0,0$	$\frac{1}{432}(2n+3)(n-1)^2$
$(0,1,0,1) (1^{--})$	$(0,1,2,1) (1^{--})$	$0,0$	$\frac{1}{540}(2n+3)(2n-5)^2$
$(0,1,0,1) (1^{--})$	$(0,1,1,0) (1^{+-})$	$1,1$	$\frac{1}{6}$
$(0,0,1,1) (0^{++})$	$(0,0,1,1) (0^{++})$	$0,0$	$\frac{1}{432}(2n+3)(n-3)^2$
$(0,1,1,1) (1^{++})$	$(0,1,1,1) (1^{++})$	$0,0$	$\frac{1}{144}(2n+3)(n-2)^2$
$(0,1,1,0) (1^{+-})$	$(0,1,1,0) (1^{+-})$	$0,0$	$\frac{1}{144}(2n+3)(n-1)^2$

by its internal quantum numbers n_ℓ, J_ℓ, L_ℓ , and S_ℓ ($\ell = 1, 2$), i.e., the internal radial excitation, total angular momentum (spin of the meson), orbital angular momentum of the $q\bar{q}$ system, and intrinsic $q\bar{q}$ spin, respectively. The relative motion of the two mesons is characterized by their relative orbital angular momentum L and total spin S , dictated by the J^{PC} quantum numbers. The relative radial excitation of the two-meson system is directly related to n (see Refs. [11] for details).

When we determine the recoupling coefficients, we find that they decrease rapidly for higher radial excitations n (see Table 1), which implies that the higher terms in the sum over n in formula (2) are suppressed.

S-wave scattering. In Fig. 2c we compare the result of formula (2) to the data of Refs. [3, 4]. We find a fair agreement for total invariant masses up to 1.6 GeV. However, we should bear in mind that the LASS data must have larger error bars for energies above 1.5 GeV than suggested in Ref. [4], since most data points fall well outside the Argand circle. Hence, for higher energies, the model should better not follow the data too precisely.

Now, in order to have some idea about the performance of formula (2) for S -wave $I = 1/2$ $K\pi$ scattering, we argue that, as in our model there is only one non-trivial eigen-phase shift for the coupled $K\pi + K\eta + K\eta'$ system, we may compare the phase shifts of our model for $K\eta$ and $K\eta'$ to the experimental phase shifts for $K\pi$. We do this comparison in Figs. 6 and 7, where, instead of the phase shifts, we plot the cross sections, assuming no inelasticity in either case. The latter assumption is, of course, a long shot. Nevertheless, we observe an extremely good agreement. In particular, for

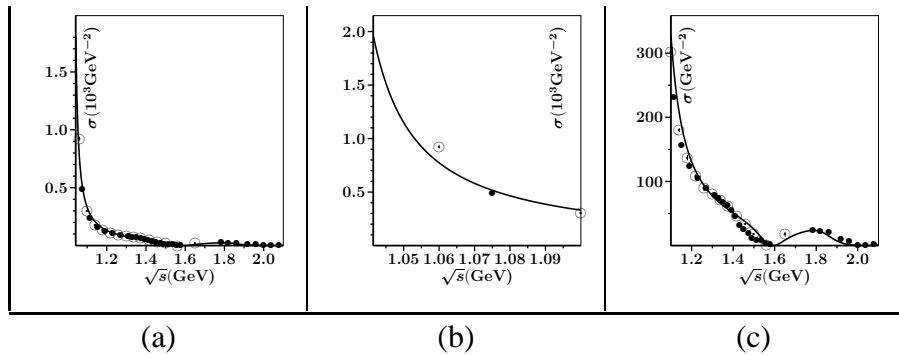


FIGURE 6. S -wave $K\eta$ ‘‘cross section’’ (see text), as a function of total invariant mass. **(a)**: From threshold up to 2.1 GeV. **(b)**: Detail for lower energy. **(c)**: Detail for higher energy. The data are taken from Ref. [3] (open circles) and Ref. [4] (full circles).

$K\eta'$ (Fig. 7) we become aware of a structure in the data at about 1.9 GeV, indicating the presence of a not-anticipated pole. This is something we would not have easily noticed from the data alone.

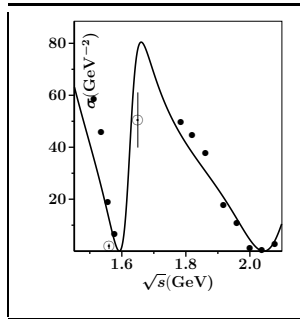


FIGURE 7. S -wave $K\eta'$ ‘‘cross section’’ (see text), as a function of total invariant mass. The data are taken from Ref. [3] (open circles) and Ref. [4] (full circles).

When we inspect formula (2) for poles in the S -wave isodoublet $K\pi$ scattering amplitude, then we find the pole structure as summarized in Table 2, i.e., five poles at energies up to about 2.2 GeV real part. The first pole, at $0.772 - 0.281i$ GeV, describes the heavily

disputed $K_0^*(800)$ structure, whereas the second pole, at $1.52 - 0.097i$ GeV, represents the well-established $K_0^*(1430)$ resonance.

TABLE 2. T -matrix poles for S -wave $K\pi$ scattering, as obtained from Eq. (2).

Pole (GeV)	$0.772 - 0.281i$	$1.52 - 0.097i$	$1.79 - 0.052i$	$2.04 - 0.15i$	$2.14 - 0.065i$
Origin	continuum	confinement	confinement	continuum	confinement

Our model is explicitly flavor-independent, meaning that the only flavor breaking in formula (2) stems from the effective quark masses which determine the ground state of the confinement spectrum (see Eq. 3), and from the masses of the mesons in the scattering channels. Consequently, $\pi\pi$ scattering is not very different from $K\pi$ scattering in our model. We may expect then that each of the two flavor combinations that couple to isoscalar S -wave $\pi\pi$ and KK scattering has a pole structure similar to the one in isodoublet $K\pi$ scattering, with the proviso that $n\bar{n}$ - $s\bar{s}$ mixing in the $I=0$ case introduces an extra complication. The to-be-expected poles are given in Table 3, alongside the f_0

TABLE 3. The left-hand table shows the real parts of the poles in the amplitude for $n\bar{n}$ (upper row) $s\bar{s}$ (lower row) S -wave $\pi\pi+KK$ coupled-channel scattering, as expected in analogy with $K\pi$ (see Table 2), whereas the right-hand table shows the observed f_0 states listed in the Tables of Particle Properties [12]. In the upper (lower) rows, we collect those resonances which we expect to be mainly $n\bar{n}$ ($s\bar{s}$).

$n\bar{n}$ (GeV)	0.66	1.42	1.69	1.94	2.04
$s\bar{s}$ (GeV)	0.86	1.62	1.89	2.14	2.24

f_0 (GeV)	0.6	1.37	1.71	2.02	2.33
f_0 (GeV)	0.98	1.50	2.20		

structures reported in experiment.

The often read comment that *too many isoscalar states are observed* [13], in order to justify the application of alternative quark, or even quarkless, configurations [14], is not confirmed here.

Most probably, mesons are just mixtures [15] of *quark-antiquark* states [16], *two-meson molecules* [17], *glueballs* [18], *tetraquarks* [19], *hexaquarks, hybrids* [20], and so forth. Here, we have shown that the first two of the latter list of possible components are the most relevant ones. Moreover, a resonance is really a collection of states, all with different masses. Each of these states will have a different composition.

In Table 4 we summarize the scalar poles which we obtained in the past [21, 22, 8]. The first four lines in the third column of Table 4 are referred to in the literature as the scalar-meson nonet [23], given by the isoscalars $f_0(600)$ and $f_0(980)$, the isotriplet $a_0(980)$, and the isodoublet pair $K_0^*(800)$ [24]. Here, they form part of the complex pole spectrum of the general scattering amplitude (1), where they appear as the lowest-lying continuum poles. The first four lines in the fourth column of Table 4 describe the nonet of scalar mesons that stem directly from the $J^P = 0^+$ ground states of the confinement spectrum.

Summary and discussion. In the foregoing, we have shown that the most relevant information on (meson) spectra amounts to the knowledge about the complex pole positions of the scattering amplitudes. Furthermore, we presented a general form of amplitudes for non-exotic hadron-hadron scattering with any possible flavor combination, based upon the most prominent properties of strong interactions, namely *quark confinement*.

TABLE 4. S-wave scattering poles for various flavor/isospin combinations with $J^P = 0^+$. In the columns “continuum”, “ground state”, and “excitation” we indicate the origin of the poles, i.e., either meson-meson continuum, or confinement spectrum (ground state or first radial excitation).

channel	$q\bar{q}$	continuum	ground state	excitation
$\pi\pi$	$n\bar{n}$	$0.47 - 0.21i$	$1.36 - 0.13i$	-
$K\pi$	$n\bar{s}$	$0.77 - 0.28i$	$1.52 - 0.10i$	$1.79 - 0.05i$
$\eta\pi$	$n\bar{n}$	$0.97 - 0.028i$	$1.45 - 0.13i$	-
$\pi\pi$	$s\bar{s}$	$0.99 - 0.020i$	$1.51 - 0.06i$	-
$D\pi$	$c\bar{n}$	$2.14 - 0.16i$	$2.58 - 0.12i$	-
DK	$c\bar{s}$	2.33	$2.80 - 0.20i$	-
$B\pi$	$n\bar{b}$	$6.06 - 0.29i$	$5.46 - 0.03i$	$6.03 - 0.05i$
BK	$s\bar{b}$	$6.21 - 0.33i$	5.61	$6.05 - 0.03i$
BD	$c\bar{b}$	$7.12 - 0.43i$	6.64	$7.11 - 0.03i$

ment, quark-pair creation, and flavor invariance. The resulting pole spectrum may very well be compared to experiment. It is true that the predicted cross sections and phase shifts are not always in very accurate agreement with the data, as could hardly be expected in view of the extremely wide scope of the model. In part this may also be due to the inaccuracy of some experimental numbers. Nevertheless, the model can be improved as well, as we suggest next.

- At present, we determine the vertices in the framework of the 3P_0 mechanism, assuming that all quark masses involved are the same. However, different quark masses can be dealt with, too. Computer programs already exist for several years, but have not yet been implemented.
- The one-delta-shell approximation “unfortunately” works too well. Hence, although it is perfectly known how to implement more complicated transition potentials [25], and even some computer code is ready, the finishing touch could still take a while, unless some extra manpower becomes available.
- The kinematics of meson pairs below threshold is most certainly not being dealt with in the most appropriate way by us. This is a subject which deserves to be studied in more detail.

Acknowledgment. One of us (EvB) wishes to thank the organizers for inviting him to the Hadron05 conference, their warm hospitality, and for organizing this great event. This work was partly supported by the *Fundação para a Ciência e a Tecnologia* of the *Ministério da Ciência, Tecnologia e Ensino Superior* of Portugal, under contract POCTI/FP/FNU/50328/2003 and grant SFRH/BPD/9480/2002.

REFERENCES

1. E. van Beveren, G. Rupp, T. A. Rijken, and C. Dullemond, Phys. Rev. D **27**, 1527 (1983).
2. E. van Beveren and G. Rupp, arXiv:hep-ph/0304105.
3. P. Estabrooks, R. K. Carnegie, A. D. Martin, W. M. Dunwoodie, T. A. Lasinski, and D. W. Leith, Nucl. Phys. B **133**, 490 (1978).
4. D. Aston *et al.*, LASS collaboration, Nucl. Phys. B **296**, 493 (1988).
5. S. Godfrey, Phys. Rev. D **72**, 054029 (2005) [arXiv:hep-ph/0508078].
6. G. Rupp, F. Kleefeld and E. van Beveren, arXiv:hep-ph/0412078.
7. S. L. Adler, arXiv:hep-ph/0505177.
8. E. van Beveren and G. Rupp, Mod. Phys. Lett. A **19**, 1949 (2004) [arXiv:hep-ph/0406242]; E. van Beveren, J. E. G. Costa, F. Kleefeld and G. Rupp, arXiv:hep-ph/0509351.
9. E. van Beveren, C. Dullemond, and G. Rupp, Phys. Rev. D **21**, 772 (1980) [Erratum-ibid. D **22**, 787 (1980)]; F. Kleefeld, AIP Conf. Proc. **717**, 332 (2004) [arXiv:hep-ph/0310320].
10. E. van Beveren, Z. Phys. C **21**, 291 (1984); E. van Beveren and G. Rupp, Eur. Phys. J. C **11**, 717 (1999) [arXiv:hep-ph/9806248]; Phys. Lett. B **454**, 165 (1999) [arXiv:hep-ph/9902301].
11. J. E. Ribeiro, Phys. Rev. D **25**, 2406 (1982); E. van Beveren, Z. Phys. C **17**, 135 (1983).
12. S. Eidelman *et al.* [Particle Data Group Collaboration], Phys. Lett. B **592**, 1 (2004).
13. Claude Amsler, Phys. Lett. B **541** (2002) 22 [arXiv:hep-ph/0206104].
14. F. E. Close, arXiv:hep-ph/0411396.
15. T. Barnes, F. E. Close, J. J. Dudek, S. Godfrey and E. S. Swanson, Phys. Lett. B **600**, 223 (2004) [arXiv:hep-ph/0407120].
16. M. R. Pennington, J. Phys. Conf. Ser. **18**, 1 (2005) [arXiv:hep-ph/0504262]; arXiv:hep-ph/0509265; M. D. Scadron and M. Nagy, arXiv:hep-ph/0507168; D. K. Hong and C. j. Song, arXiv:hep-ph/0407274.
17. A. H. Fariborz, R. Jora, and J. Schechter, Phys. Rev. D **72**, 034001 (2005) [arXiv:hep-ph/0506170]; L. Roca, E. Oset and J. Singh, Phys. Rev. D **72**, 014002 (2005) [arXiv:hep-ph/0503273]; T. Kunihiro, arXiv:hep-ph/0407355; M. F. M. Lutz and E. E. Kolomeitsev, arXiv:hep-ph/0406015; P. Bicudo, Nucl. Phys. A **748**, 537 (2005) [arXiv:hep-ph/0401106].
18. A. H. Fariborz, AIP Conf. Proc. **688**, 154 (2004); Int. J. Mod. Phys. A **19**, 5417 (2004); T. Teshima, I. Kitamura, and N. Morisita, AIP Conf. Proc. **619**, 487 (2002).
19. M. Napsuciale and S. Rodriguez, Phys. Rev. D **70**, 094043 (2004) [arXiv:hep-ph/0407037]; Phys. Rev. D **71**, 074008 (2005) [arXiv:hep-ph/0411150]; J. R. Pelaez, Mod. Phys. Lett. A **19**, 2879 (2004) [arXiv:hep-ph/0411107]; T. V. Brito, F. S. Navarra, M. Nielsen, and M. E. Bracco, Phys. Lett. B **608**, 69 (2005) [arXiv:hep-ph/0411233].
20. Farida Iddir and Lahouari Semlala, arXiv:hep-ph/0211289.
21. E. van Beveren *et al.*, Z. Phys. C **30**, 615 (1986).
22. E. van Beveren and G. Rupp, Eur. Phys. J. C **22**, 493 (2001) [arXiv:hep-ex/0106077]; arXiv:hep-ph/0312078.
23. M. M. Nagels, T. A. Rijken, and J. J. de Swart, Phys. Rev. D **20**, 1633 (1979); M. D. Scadron, Phys. Rev. D **26**, 239 (1982); A. V. Anisovich and A. V. Sarantsev, Phys. Lett. B **413**, 137 (1997) [arXiv:hep-ph/9705401]; T. Ishida, M. Ishida, S. Ishida, K. Takamatsu, and T. Tsuru, in *Upton 1997, Hadron Spectroscopy*, pp. 385–388 [arXiv:hep-ph/9712230]; D. Black, A. H. Fariborz, F. Sannino, and J. Schechter, Phys. Rev. D **59**, 074026 (1999) [arXiv:hep-ph/9808415]; A. H. Fariborz and J. Schechter, Phys. Rev. D **60**, 034002 (1999) [arXiv:hep-ph/9902238]; M. Ishida, arXiv:hep-ph/9905259; D. Black, A. H. Fariborz, and J. Schechter, in *Kyoto 2000*, p. 115 [arXiv:hep-ph/0008246]; N. A. Törnqvist, arXiv:hep-ph/0201171; I. Bediaga [Fermilab E791 collaboration], arXiv:hep-ex/0208039; M. Ishida, AIP Conf. Proc. **688**, 18 (2004); M. Ablikim *et al.* [BES Collaboration], arXiv:hep-ex/0506055; J. A. Oller, AIP Conf. Proc. **688**, 167 (2004); D. M. Li, K. W. Wei, and H. Yu, Eur. Phys. J. A **25**, 263 (2005) [arXiv:hep-ph/0507121]; Y. B. Dai and Y. L. Wu, Eur. Phys. J. C **39**, S1 (2005) [arXiv:hep-ph/0304075]; D. V. Bugg, arXiv:hep-ex/0510014; arXiv:hep-ex/0510021; G. Erkol, R. G. E. Timmermans, and T. A. Rijken, Phys. Rev. C **72**, 035209 (2005).
24. E. M. Aitala *et al.* [E791 Collaboration], Phys. Rev. Lett. **89**, 121801 (2002) [arXiv:hep-ex/0204018]; C. Göbel, on behalf of the E791 Collaboration, in *Rio de Janeiro 2000, Heavy quarks at fixed target*, pp. 373–384 [arXiv:hep-ex/0012009]; AIP Conf. Proc. **619**, 63 (2002) [arXiv:hep-ex/0110052].
25. C. Dullemond, G. Rupp, T. A. Rijken, and E. van Beveren, Comput. Phys. Commun. **27**, 377 (1982).